J. Phys. A: Math. Gen. 26 (1993) 477–493. Printed in the UK

Exact multicritical behaviour of the Potts model

Bernard Nienhuis†, S Ole Warnaar† and Henk W J Blöte‡

† Instituut voor Theoretische Fysica, Universiteit van Amsterdam, Valckenierstraat 65, 1018 XE Amsterdam, Netherlands

‡ Laboratorium voor Technische Fysica, Technische Universiteit Delft, Postbus 5046, 2600 GA Delft, Netherlands

Received 24 July 1992

Abstract. A two-dimensional q-state Potts model with vacancies and four-spin interactions is studied. The parameter space of the model contains a critical and a tricritical manifold. Moreover for $0 \leqslant q \leqslant 9/4$ a multicritical point is found which is the locus where the tricritical transition changes from first- to second-order. At this multicritical point, which can be located exactly, the model is solvable. We compute the value of the central charge and a number of critical exponents.

1. Introduction

The classification of second-order phase transitions in types as critical, tricritical etc. is usually done on the basis of the number of coexisting phases that become critical. This is not convenient for the q-state Potts model, in which q-phase coexistence terminates at the transition point. For $q \leqslant 4$, when the transition is continuous, it is usually termed a critical point.

When neutral states are introduced in the Potts model [1], the second-order transition may become first-order, as the weight of these neutral states is increased, at what is then called the tricritical point. In this paper we further generalize this dilute Potts model with four-spin interaction and find a transition at which the tricritical point itself turns first-order. This new multicritical transition relates to the tricritical point just like the tricritical to the critical point. For lack of better designation we will refer to it as tri^{2}critical.

A further clarification of this phenomenon may well be given by viewing this hierarchy of criticality in light of the order parameter. Let s be one of the spin variables, which assumes one of the values $\{1, 2, \ldots, q\}$. For the order parameter we may take

$$M = \langle q\delta_{s,1} - 1 \rangle . \tag{1}$$

In the high-temperature disordered phase this probability strictly vanishes. In the low-temperature ordered phase M deviates from zero. When $q \leqslant 4$ the order parameter of the Potts model in the ordered phase vanishes continuously as the critical point is approached. When vacancies are introduced into the model the transition may be first-order even for $q \leqslant 4$. Then the value of M is discontinuous at the transition. At the tricritical point itself, where the transition changes from first- to second-order,

0305-4470/93/030477+17$07.50

the order parameter vanishes continuously. When the tricritical point is approached along the first-order transition, the jump in the order parameter approaches zero continuously. However, we now propose the possibility that the magnitude of the discontinuity in the order parameter remains non-zero even up to the point where the transition becomes second-order, where it jumps to zero: the 'tricritical' transition itself has turned first-order.

Not only do we find the locus of the tri^{2}critical transition exactly, we also find that the model is solvable at this point, just as the ordinary Potts model is solvable at its critical point. In this paper we present the value of the central charge and of several critical exponents for the tri^{2}critical point as a function of q. It turns out that the relation between the central charge and the critical exponents, does not follow the Kac formula except at special values of q. This is distinct from the known exponents of e.g. the critical and tricritical point of the Potts model, which agree with the Kac formula even at non-integer values of q.

The generalized Potts model we consider here has been discussed before [2], but the phenomenon that the tricritical transition may be driven first-order, and the solvability of the model has not been observed previously.

2. The model

Consider the ordinary Potts model [3] on the square lattice $\mathcal{L}$. Its Hamiltonian is

$$-\beta\mathcal{H} = J \sum_{<i,j>} \delta_{s_i,s_j} \tag{2}$$

in which the variables s take values from $\{1, 2, \ldots, q\}$, and the summation is over nearest neighbour pairs of sites. This model has a transition between an ordered phase at large coupling constant J and a disordered phase at small J. This transition is first-order when $q > 4$ and second-order for $q \leqslant 4$ [4]. Since in high- or low-temperature expansions of the partition sum the number of states plays the role of a free parameter, q is usually not restricted to the natural numbers.

In an attempt to unify the description of the first- and second-order transitions the model has been generalized [1] to the dilute Potts model, in which each site is either empty or occupied with a variable which assumes one of q values, i.e. each site can be in one of $q+1$ states. The Hamiltonian reads

$$-\beta\mathcal{H} = J \sum_{<i,j>} v_i v_j \delta_{s_i,s_j} + K_1 \sum_i (1-v_i) + K_2 \sum_{<i,j>} (1-v_i)(1-v_j). \tag{3}$$

Here the variables v are zero or one for the vacant or occupied sites respectively. In this model the transition for $q \leqslant 4$ can be both first- (for large K_1) and second-order (for small K_1), separated by what is called a tricritical point. It has turned out [1, 2, 5] that the exponents of the critical point and those of the triciritical point are two branches of the same function of q which is analytic for $q < 4$ and has a branch point at $q = 4$.

The original Potts model (2) exhibits a dual symmetry [3] between the low- and high-temperature phase, by means of which the critical point is easily located. Moreover, at the critical point the model is solvable [4]. These properties appear to be lost for the dilute Potts model. Therefore we now generalize the dilute Potts

model, thus restoring the dual symmetry, with the hope of finding a solvable tricritical point. We propose the following Hamiltonian

$$\exp(-\beta\mathcal{H}) = \prod_{\mu}\left[f_\mu + (1-f_\mu)\delta_{s_i,s_j}\delta_{s_j,s_k}\delta_{s_k,s_l}\delta_{s_l,s_i}v_iv_jv_kv_l\right]$$
$$\times \exp\left\{\sum_{<i,j>}\left[Jv_iv_j\delta_{s_i,s_j} + K_2(1-v_i)(1-v_j)\right] + K_1\sum_i(1-v_i)\right.$$
$$\left. + M_1\sum_\mu(1-f_\mu) + M_2\sum_{<\mu,\nu>}(1-f_\mu)(1-f_\nu)\right\}. \tag{4}$$

The summations and product run over the sites, links and faces of the lattice. The faces are labelled with Greek indices, and in the product it is assumed that the face μ is immediately surrounded by the four sites i, j, k and l. This model has besides occupation variables v and Potts variables s also plaquette variables f taking the values zero or one. In the absence of the interaction coefficient M_2 these variables may be summed out, resulting in a pure four-spin interaction with strength $\ln[\exp(M_1)+1]$. The dual transformation is a trivial generalization of that of the ordinary Potts model. While keeping the configuration of v and f fixed, the dual transformation may be performed on the remaining variables s. The dual model has the same form, with the role of f and v interchanged. We will show below that this model is equivalent to that defined and studied in [2].

3. Equivalent loop model

In this section we will consider a different representation of the model (4). Via a random cluster expansion we map the model onto a loop model, for which we will solve the Yang–Baxter (YB) equation [6]. This yields a solvable manifold in the space spanned by q and the coupling constants J, K_1, K_2, M_1 and M_2. Another representation, as an 'interaction-round-a-face' (IRF) model of the Temperley–Lieb type, will be discussed in appendix B.

In order to write the above model as a loop model, we will first make a generalized random cluster expansion [7]. For this purpose the partition function of the model is written as

$$Z = \sum_{\{f,s,v\}}\prod_i\left[v_i + (1-v_i)e^{K_1}\right]\prod_{<i,j>}e^{K_2(1-v_i)(1-v_j)}\left[1 + v_iv_j\delta_{s_i,s_j}(e^J-1)\right]$$
$$\times\prod_\mu\left[f_\mu + v_iv_jv_kv_l\delta_{s_i,s_j}\delta_{s_j,s_k}\delta_{s_k,s_l}(1-f_\mu)e^{M_1}\right]\prod_{<\mu,\nu>}e^{M_2(1-f_\mu)(1-f_\nu)}. \tag{5}$$

The summation over a spin variable s is performed only when the corresponding site is occupied, i.e. $v=1$. We expand the binomial products, so that each term in the expansion has, apart from multiplicative factors, two possible weights for each site, edge and face of the lattice.

(1) For a site we either have the term v or the term $(1-v)e^{K_1}$, represented graphically by leaving the site empty or placing a dot on the site, respectively.

(2) For a face we either have the term f or the term $vvvv\delta\delta\delta(1-f)e^{M_1}$, represented graphically by leaving the face empty or placing a dot on the face and bonds on the surrounding edges. These edges give a factor e^J.
(3) For the remaining edges we either have the term $vv\delta(e^J-1)$ or 1, represented graphically by placing a bond on the edge or leaving it empty.

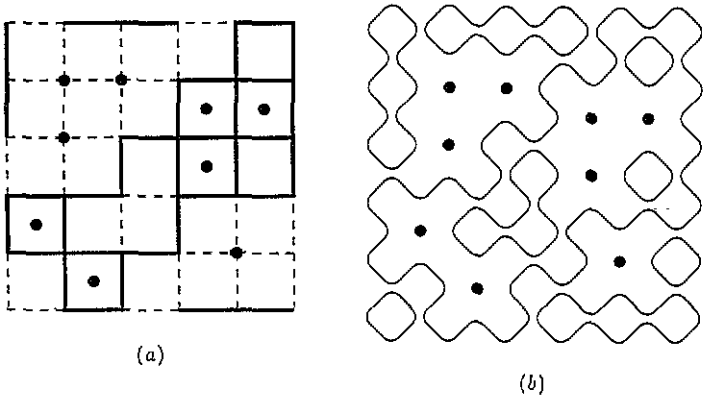

Figure 1. (*a*) Graph of the random cluster expansion of (5), and (*b*) polygon decomposition of the same graph.

Each term in the expansion is now represented by a graph on the lattice consisting of bonds and dots. An example is shown in figure 1(*a*). The sites of the lattice are now partitioned into connected components, or clusters, such that sites connected by a bond belong to the same cluster. We can now sum over $\{f,s,v\}$ trivially. In fact, the distribution of dotted sites and faces fixes $\{f\}$ and $\{v\}$ completely and we only have to sum over $\{s\}$, yielding a factor $q^{N_c-N_v}$, where N_c is the number of connected components and N_v the number of dotted sites.

As a result we find that the partition function can be written as the sum over all graphs $G_{\mathcal{L}}$ on $\mathcal{L}$ consisting of dotted sites and faces and of edges covered by bonds, with the restriction that dotted sites (faces) are surrounded by four empty (covered) edges.

$$Z=\sum_{G_{\mathcal{L}}} e^{J(4N_f-P_f)+K_1N_v+K_2P_v+M_1N_f+M_2P_f}(e^J-1)^{N_b-4N_f+P_f}q^{N_c-N_v} \tag{6}$$

where N_f is the number of dotted faces, N_b the number of bonds and P_v (P_f) are the number of nearest-neighbour pairs of dotted sites (faces).

We now split the summation in (6) into two parts. First we fix the dots. This also fixes the states of the edges surrounding these dots. Then we sum over all the possible graphs $G_{\mathcal{M}}$ consisting of bonds on the remaining edges, which form the reduced lattice $\mathcal{M}$. Finally we sum over all dot configurations

$$Z=\sum_{\text{dots}} e^{J(4N_f-P_f)+K_1N_v+K_2P_v+M_1N_f+M_2P_f}\sum_{G_{\mathcal{M}}}(e^J-1)^{N_b-4N_f+P_f}q^{N_c-N_v}. \tag{7}$$

From this expression it is clear that this model is equivalent to the one studied in [2].

Baxter *et al* [8] have shown how a Potts model on an arbitrary planar lattice can be written as a dense loop model, by making a polygon decomposition of its

surrounding or medial lattice. The second summation in the above expression is the partition function of such a Potts model, on the lattice $\mathcal{M}$. Therefore we can readily use their result to write this part of the partition function as a loop model on the medial lattice $\mathcal{M}'$ of $\mathcal{M}$

$$Z = q^{N/2}\sum_{\text{dots}} e^{J(4N_t-P_t)+K_1N_v+K_2P_v+M_1N_t+M_2P_t} q^{(P_t-N_v-3N_t)/2} \sum_{G_{\mathcal{M}'}} \rho_1^{n_1}\rho_2^{n_2}q^{p/2}. \quad (8)$$

The second sum is over all configurations consisting of closed non-intersecting loops on $\mathcal{M}'$, n_1, n_2 and ρ_1, ρ_2 are the number and Boltzmann weights of the vertices 1 and 2, of figure 2 and p is the number of loops. The variable N_c has been eliminated by $2N_c = N - N_b + p + N_v + N_t$, N being the total number of sites of $\mathcal{L}$. The weights ρ_1 and ρ_2 are given by

$$\rho_1 = 1 \qquad \rho_2 = \frac{e^J - 1}{\sqrt{q}}. \quad (9)$$

Each term in the set of bond graphs $G_{\mathcal{M}}$ corresponds to one of the polygon decompositions $G_{\mathcal{M}'}$, as shown in figure 1(*b*).

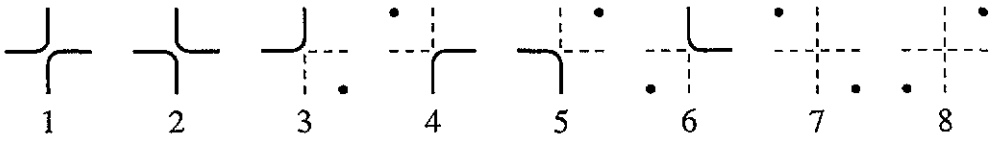

Figure 2. The eight vertices of the loop model. The edge of $\mathcal{L}$ runs in the NW–SE direction.

To account for the configuration and the weight of the dots, we extend the loop model on $\mathcal{M}'$ to a generalized loop model on the medial lattice $\mathcal{L}'$ of $\mathcal{L}$ by including the vertices $3, \ldots, 8$ of figure 2.

$$Z = q^{N/2}\sum_{G_{\mathcal{L}'}} \rho_1^{n_1} \ldots \rho_8^{n_8} q^{p/2} \quad (10)$$

where

$$\begin{aligned} \rho_3 &= \rho_4 = q^{-1/8}e^{K_1/4} & \rho_7 &= q^{-1/4}e^{K_1/2+K_2} \\ \rho_5 &= \rho_6 = q^{-3/8}e^{J+M_1/4} & \rho_8 &= q^{-1/4}e^{J+M_1/2+M_2}. \end{aligned} \quad (11)$$

It is in this simple loop representation that we seek a solvable subspace of the model. In appendix A we discuss the concept of YB equations for loop models and apply this to the loop model (10). The solution we find, at the isotropic point and up to a gauge transformation, is

$$\begin{aligned} &\rho_1 = \rho_2 = 1 && q = (\Delta - \Delta^{-1})^2 \\ &\rho_3 = \rho_4 = \rho_5 = \rho_6 = \Delta^{-1/4} && \Delta = 2\cos\lambda \\ &\rho_7 = \rho_8 = \Delta^{1/2} + \Delta^{-1/2}. \end{aligned} \quad (12)$$

If we express the parameters of our model in terms of this solution, we find

$$\begin{aligned} e^{J} &= q^{1/2}+1 \qquad & e^{M_1} &= \Delta^{-1}q^{3/2}(q^{1/2}+1)^{-4} \\ e^{K_1} &= \Delta^{-1}q^{1/2} & e^{M_2} &= (\Delta+1)(q^{-1/2}+1) \\ e^{K_2} &= (\Delta+1). \end{aligned} \tag{13}$$

When $\Delta \geqslant 1$ these parameters correspond to positive Boltzmann weights for the Potts model. However positivity of the Boltzmann weights is not a condition for solvability, and we may define other non-physical branches of solvable models with the same value of q

branch	
1	$1 \leqslant \Delta \leqslant 2$
2	$0 \leqslant \Delta \leqslant 1$
3	$-1 \leqslant \Delta \leqslant 0$
4	$-2 \leqslant \Delta \leqslant -1$.

(14)

4. Central charge and exponents

In this section we give analytical expressions for the central charge and some exponents of the model as defined by (4) and (13). The results, which are confirmed below by numerical data, turn out to be in contrast with the Kac formula, which, for unitary models, relates the central charge to critical exponents.

For unitary models with central charge $c < 1$ parameterized by [9]

$$c = 1 - \frac{6}{h(h-1)} \qquad h = 4,5,6,\ldots \tag{15}$$

the critical exponents are given by [10]

$$x = \frac{[hr-(h-1)s]^2-1}{2h(h-1)} \qquad 1 \leqslant s \leqslant r \leqslant h-2. \tag{16}$$

When the ordinary Potts model is generalized to a non-natural number of states q, e.g. in the random cluster formulation, it is in general not unitary. Even so, when the central charge is parametrized by (15) the exponents are still given by (16) in which the indices r and s take fixed integer values or are linear in h. The same is true for exponents of the O(n) model with general values of n [11].

In order to calculate the central charge and exponents for the model (4) with (13) we use an alternative representation as a Temperley–Lieb model. From the construction of these models as given in appendix B, it is apparent that they are equivalent to a large family of models, which includes the symmetric six-vertex model. For the latter the central charge c and some of the critical exponents x have been computed. They are given by (B8)–(B10)

$$c = 1 - \frac{6}{h(h-1)} \qquad \text{and} \qquad x = \frac{k^2-1}{2h(h-1)} \tag{17}$$

with h and k given by Δ and Δ' as

$$\Delta = 2\cos\frac{\pi}{h} \qquad \text{and} \qquad \Delta' = 2\cos\frac{k\pi}{h}. \tag{18}$$

The possible values of Δ and Δ' are

$$\begin{aligned} &(\Delta - \Delta^{-1})^2 = q \\ &\Delta' \in \{1/\Delta, -1/\Delta, -\Delta, 1, -1\}. \end{aligned} \tag{19}$$

The first three choices for Δ' yield thermal exponents, and the last two magnetic exponents. It is clear that for general Δ the parameter k is non-integer, as required by (16).

Because the disagreement with the Kac formula (16), for values of q other than 1 and 2, is quite striking we have also constructed the transfer matrix on a cylinder with a circumference of L sites. The construction of the transfer matrix and analysis of its eigenvalues are explained in [24]. The eigenvalues are computed numerically, not only for the physical branch 1, but also for the other branches (14), in which some of the Boltzmann weights are negative. From conformal invariance [12] it follows that they have the form

$$\Lambda_L^{(j)} = \exp\left[Lf_\infty + \frac{\pi c_j}{6L} + o\left(\frac{1}{L}\right)\right]. \tag{20}$$

The value of the bulk free energy f_∞ is known from the equivalence (appendix B) to the six-vertex model [13]. Thus the amplitudes c_j of the leading finite size corrections can be estimated from the numerical eigenvalues. The central charge c is the amplitude, say c_0, of the largest eigenvalue and the critical exponents are given by $x_j = (c_0 - c_j)/12$.

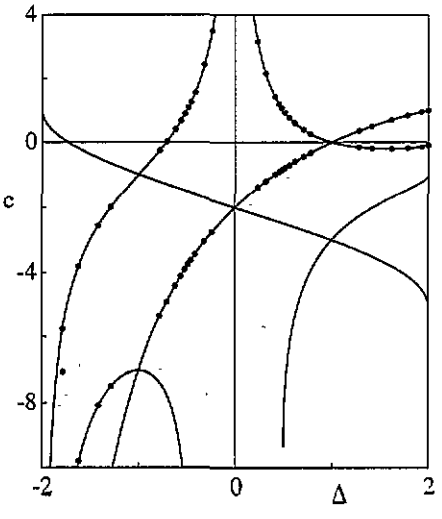

Figure 3. The finite size amplitude of the eigenvalues of the transfer matrix. The dots indicate the numerical results of the largest two eigenvalues, and the curves the theoretical predictions for the symmetric eigenvalues.

In figure 3 the amplitudes of the finite size corrections of the largest two symmetric eigenvalues of the transfer matrix are shown together with the theoretical formulae (17) for c and $c - 12x$. The numerical data agree excellently with the theoretical amplitudes. The finite-size amplitude that runs from $c = 1$ at $\Delta = -2$ down to $c = -5$ at $\Delta = 2$ is associated with a change of sign between the states on the sites and the faces of the lattice. However, since the interchange of the sites and the faces is not taken into account in the numerical calculation, this eigenvalue does not come out of the computation. When that theoretical amplitude is disregarded, the numerical data in each branch correspond to the largest two of the remaining amplitudes.

The accuracy is very good, not only in the region where $\Delta > 1$ is indeed the largest eigenvalue of the adjacency matrix, but also in the analytic continuation where Δ can be any of the four eigenvalues. Remarkably, the agreement does not even deteriorate when the parameter k in (18) is imaginary.

In the ordinary Potts model the phase transition changes from second- to first-order when $q = 4$. We see a similar phenomenon in this generalized Potts model but now at $q = 9/4$, where $\Delta = 2$. For larger values of q the equations (17) and (18) admit no real value of the central charge. Apparently the solvable model is not critical at these values of q.

Curiously the non-physical branches with $-1 < \Delta < 1$ do not have such a cut-off in q but continue to be critical for arbitrarily large values of q.

From the above results it is clear that the new solvable Potts model is not at its tricritical point. In the next section we discuss the nature of this new critical point of the Potts model.

5. The phase diagram

The role of the critical point (13) becomes more apparent when the self-dual plane is considered. As explained in [2] the partition sum of the model (4) is invariant under a dual transformation

$$\begin{aligned} &e^{\tilde{J}} - 1 = q/(e^J - 1) \qquad && e^{\tilde{M}_1} = q^3 e^{K_1}/(e^J - 1 + q)^4 \\ &e^{\tilde{K}_1} = q e^{M_1}/(1 - e^{-J})^4 \qquad && e^{\tilde{M}_2} = e^{K_2}(e^J - 1 + q)/q \\ &e^{\tilde{K}_2} = e^{M_2}(1 - e^{-J}). \end{aligned} \tag{21}$$

The self-dual subspace can be conveniently parametrized by means of the weights of the corresponding loop model (11), with

$$\rho_1 = \rho_2 \qquad \rho_3 = \rho_4 = \rho_5 = \rho_6 \qquad \rho_7 = \rho_8 \tag{22}$$

of which, with an overall normalization, two are independent. In the loop model the dual transformation is simply an exchange of the two sublattices, corresponding to the sites and faces respectively of the original Potts model. In the ordered phase of the Potts model there exist an infinite cluster of sites, in which small clusters of faces are separated by small loops. In the disordered phase, the sites form small clusters circumscribed by loops inside an infinite cluster of faces. At the phase transition

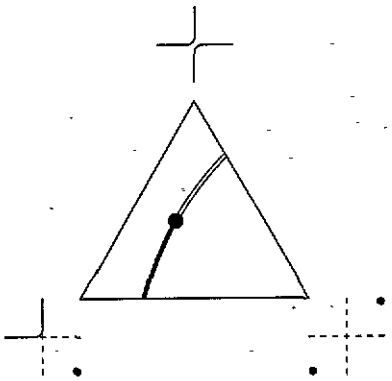

Figure 4. Schematic phase diagram in the self-dual plane.

between the ordered and disordered phase the loops separating the clusters of faces and sites tend to be very long. The vacancies and dotted faces act in this description as loops around elementary plaquettes.

Figure 4 gives a sketch of a plausible phase diagram, within the self-dual plane, which itself constitutes the phase transition between the ordered and disordered phases of the generalized Potts model. In the upper corner, when only ρ_1 and ρ_2 differ from zero, the model is reduced to the ordinary critical Potts model. In the right-hand corner, where only ρ_7 and ρ_8 differ from zero, the loop version of the model has only two states: either all faces or all sites carry dots. In this limit the model is clearly at a first-order transition with an infinite surface tension. The critical region and the first-order region of the self-dual plane are separated by a tricritical curve indicated in the figure. Part of this curve will be in the known universality class of the tricritical Potts model. However, near the right-hand boundary of figure 4, the 'tricritical' transition cannot be second-order, since the surface tension between the critical phase and the coexisting first-order phases can be made arbitrarily large. Thus we conclude, as the simplest scenario that the phase boundary between the critical and first-order regimes of the self-dual plane, is itself separated into a second-order and first-order segment, indicated in the figure by a fat and a double line respectively. We propose that the new multicritical point described in the previous sections, separates these two segments. If this description is correct the new multicritical point is related to the tricritical point just as the tricritical to the critical point; hence the name tri^2-critical point.

A further investigation into the self-dual plane, and the nature of the phase transitions is reported in [24].

6. Summary and discussion

In this paper we have introduced a generalization of the dilute Potts model. Though the parameter space contains the tricritical transition of the dilute Potts model, the tricritical model does not appear to be solvable.

The generalized Potts model defined here has some properties in common with the ordinary Potts model, in particular it admits a duality transformation in its parameter space, and it is solvable at a point in the self-dual subspace. At this new solvable point the model is critical only for $q \leqslant 9/4$. We calculate the central charge and

critical exponents, both numerically and analytically. In contrast to the ordinary q-state Potts model the central charge and the critical exponents are not related by the Kac formula (15) and (16) for general q. Only for $q = 1$ and $q = 2$, when the model becomes identical to the A_4 and E_6 Temperley–Lieb models [19], this relation is recovered. We argue that this new solvable Potts model is multicritical and it is located where the tricritical phase transition changes from first- to second-order. This role in the phase diagram is verified in [24].

Since the new multicritical transition is related to the tricritical point just as the tricritical to the critical point, we denote it as tri^{2}critical. We suggest that the critical, tricritical and tri^{2}critical transitions are the first three of a hierarchy of tri^{n}critical points in generalized Potts models. The tri^{n}critical point is then the locus in the phase diagram where the tri^{n-1}critical transition is turned first-order. We note that the critical Potts model may be constructed as a Temperley–Lieb model from an adjacency diagram like figure B1, with all $q + 1$ legs reduced by one site. A solvable tricritical point may be viewed as an analytic continuation in q, and can in fact be constructed by a similar method [14–16], based on the same adjacency diagram, but a different loop model. This alternative construction yields solvable specimens of both the critical and the tricritical point.

On the basis of these observations we propose that the solvable models constructed from an adjacency diagram like figure B1, generalized such that the single leg to the left contains n states and the q legs to the right $n + 1$, are precisely the tri^{2n}critical and tri^{2n+1}critical points introduced above. They constitute a second-order transition for $0 \leqslant q \leqslant [(n + 2)/(n + 1)]^2$.

Acknowledgment

This research is part of the research program of FOM (Stichting voor Fundamenteel onderzoek der Materie), which is financially supported by NWO (Nederlandse Organisatie voor Wetenschappelijk Onderzoek).

Appendix A. Yang–Baxter equations for loop models

The essential difference between an ordinary vertex model and a loop model [17] is that for the latter the total weight of a configuration cannot be written as a product of local weights, each dependent only on variables in a restricted section of the lattice. In (8) the weight depends on the number of polygons p via $q^{p/2}$, so that each polygon contributes a factor $q^{1/2}$. When in a single vertex two loop segments are cut and joined again in a different way, by replacing vertex 1 by 2 of figure 2, p may be either increased or decreased by 1. Only by inspecting the entire polygons of which the segments are part, can one decide in which way p changes.

It is of course well known how to circumvent this non-locality. By making use of a simple topological property of a closed loop, any non-intersecting loop model can be mapped onto a vertex model [8]. The disadvantage of this approach however, is that the total number of vertex states of the model is significantly larger than the number of states in the loop model, resulting in a larger number of YB equations with more unknowns. Moreover, for loop models in which intersections are allowed, a transformation to a local model is generally not possible. The question therefore is:

can we, despite its global properties, define a purely local condition for two transfer matrices T and T' to commute?

The partition sum of a local model on a finite lattice may be computed by dividing the lattice in two pieces, say $\mathcal{P}$ and $\mathcal{Q}$. The partition sum of the whole is now the product of the partition sums of the pieces, summed on the states of the variables on the common boundary

$$Z_{\mathcal{P}+\mathcal{Q}} = \sum_{\alpha,\beta} Z_{\mathcal{P}}(\alpha) Z_{\mathcal{Q}}(\beta) \delta_{\alpha\beta}. \tag{A1}$$

It is this principle that allows the definition of a transfer matrix. The partition sum of a lattice is thus built up by repeatedly adding a row of vertices to an exisiting sequence. The Boltzmann weight of the rows already present only depends on the states of the last row of edges.

A generalization to a loop model is possible by the following redefinitions. The symbols α and β, which we will now refer to as connection states, determine not only (i) the state of the local variables on the boundary, e.g. which of the boundary edges are occupied by polygons, but also (ii) how the occupied boundary edges are mutually connected in the interior of the lattice. The $\delta_{\alpha\beta}$ is replaced by another symbol, say $d(\alpha,\beta)$, which is non-zero only if the local states of α and β are the same and then it takes the value of the loop fugacity raised to the number of polygons that are closed by the merging of $\mathcal{P}$ and $\mathcal{Q}$. Obviously this number is completely determined by the two connection states.

It is this prescription that has allowed the definition of a transfer matrix for loop models [18]. Multiplication of a transfer matrix corresponds to the fusion of a finite rectangular lattice with an additional row of vertices. The same principle of connection states may be applied to the definition of the YB equation. The external edges and faces of both members of the equation are the boundary of a small lattice. There is an algebraic equation on the vertex weights for each connection state of these external elements. The weight of each of the possible terms in the equation is the product of vertex weights and the loop fugacity for each loop that is closed in the interior.

A graphical representation of a typical example of an equation, for the loop model (10), is shown in figure A1.

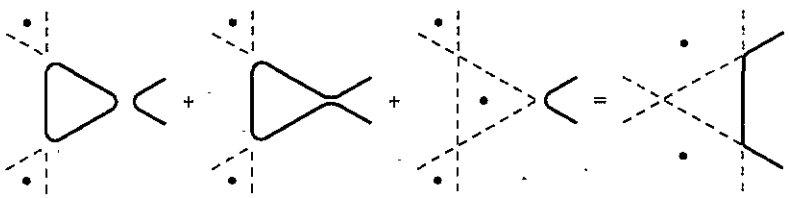

Figure A1. The equation $q^{1/2}\rho_6\rho'_4\rho''_2 + \rho_6\rho'_4\rho''_1 + \rho_8\rho'_7\rho''_6 = \rho_4\rho'_6\rho''_7$ in graphical representation.

Solving the YB equation for this model yields the following result

$$\rho_1 = \rho_3 = \rho_4 = \frac{\sin(\lambda - u)}{\sin\lambda} \qquad \rho_2 = \frac{\sin u}{\sin\lambda} \qquad \rho_5 = \rho_6 = \left(\frac{\sin\lambda}{\sin 2\lambda}\right)^{1/2} \rho_2 \tag{A2}$$

$$\rho_7 = \frac{\sin(\lambda + u)}{\sin\lambda} \qquad \rho_8 = \frac{\sin(2\lambda - u)}{\sin 2\lambda} \qquad q = \left(\frac{\sin 3\lambda}{\sin 2\lambda}\right)^2 .$$

The crossing parameter λ controls the loop fugacity, u governs the spatial anisotropy, the isotropic point being at $u = \lambda/2$. The YB equations are satisfied for $u'' = u - u'$ and $\lambda = \lambda' = \lambda''$.

Appendix B. Construction of solvable model

An alternative way to construct the solvable manifold of the generalized Potts model is the method followed by Pasquier [19, 20] and Owzarek and Baxter [21]. Below we will give the main ingredients in the construction.

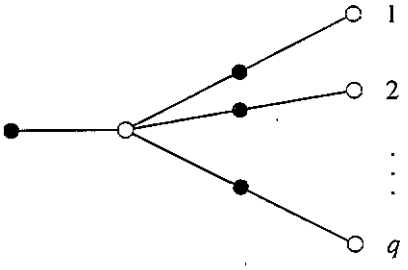

Figure B1. The adjacency diagram. The solid disks represent the possible states of the sites, and the open circles those of the faces. The leftmost disk corresponds to the vacancy, and the disks on the branches to the right the q spin states. The central branch point and the terminals of the branches correspond to the $f = 1$ and $f = 0$ faces respectively.

The first step is the observation that the variables of the model, both at the sites and the faces, may be represented as the vertices of a simple adjacency diagram $\mathcal{A}$, shown in figure B1. The rule is that each face and site of the lattice takes a value corresponding to a vertex of $\mathcal{A}$, with the restriction that a combination of a face and an adjacent site take values which are adjacent on $\mathcal{A}$. By this rule the sites and faces of the lattice automatically take values from different non-overlapping subsets of $\mathcal{A}$. The site values are the vacant state at the end of the short leg, and the midpoints of the q longer legs corresponding to the states $s = 1, \ldots, q$. The faces take the value $f = 1$, corresponding to the central branch point of the diagram, or $f = 0$, the end-point of each of the longer legs. Thus the sites around a face with $f = 0$ must all be occupied and have the same spin value, as required by the product in (4). It is not difficult to see that the configurations thus constructed correspond to the configurations of the model (4). Once the identification of the configurations of the model with an adjacency diagram has been made, the definition of the model closely follows Pasquier [19, 20], Owzarek and Baxter [21] and Foda and Nienhuis [22]. We will follow the convention of referring to the vertices of the adjacency diagram as heights.

The diagram $\mathcal{A}$ may be represented by means of the adjacency matrix A, of which the indices take heights on $\mathcal{A}$. The matrix element A_{ab} is one if a and b are adjacent on $\mathcal{A}$, and zero otherwise. The largest eigenvalue of A we denote by Δ, and the corresponding eigenvector elements as S_a.

The Boltzmann weight is given by the product over all elementary plaquettes each consisting of two neighbouring sites and faces, of the expression

$$W\begin{pmatrix} d & c \\ a & b \end{pmatrix} = \left[\delta_{ac}\left(\frac{S_b S_d}{S_a S_c}\right)^{1/4} + \delta_{bd}\left(\frac{S_a S_c}{S_b S_d}\right)^{1/4}\right] A_{ab}A_{bc}A_{cd}A_{da}. \tag{B1}$$

The variables a, b, c, d live on the sites and faces of the lattice and take heights in $\mathcal{A}$. The powers on the eigenvectors differ slightly from those in the references [19, 20, 22], such that the weights are completely isotropic. This variation corresponds to a gauge transformation which does not affect the Boltzmann weight of the entire configuration.

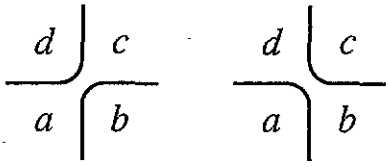

Figure B2. Graphical representation of the two terms in the local Boltzmann weight of the Temperley–Lieb models. The weight is only non-zero when the height variables not separated by lines take the same value.

The partition sum of the model is the sum over all possible configurations of the product of the local Boltzmann weights. The product may be expanded by selecting for each plaquette one of the terms of (B1), graphically represented as in figure B2. Thus each term in the expansion partitions the lattices by means of closed polygons into connected regions. All the sites or faces in the same connected region must take the same height in $\mathcal{A}$, as a result of the δ symbols in (B1). The total Boltzmann weight, which still depends on the heights actually assumed in each of the regions, can be factorized into contributions associated with each polygon [19, 22].

First the local weight for each single plaquette is split as follows

$$\delta_{ac}\left(\frac{S_b S_d}{S_a S_c}\right)^{1/4} A_{ab}A_{bc}A_{cd}A_{da} = \left[\delta_{ac}\left(\frac{S_b}{S_a}\right)^{1/4} A_{ab}A_{bc}\right] \times \left[\delta_{ac}\left(\frac{S_d}{S_c}\right)^{1/4} A_{cd}A_{da}\right]. \tag{B2}$$

These two factors are associated with the two polygon segments that pass through the plaquette. Now we have to make a distinction between polygons that are contractible to a point, and those that wind around the torus or cylinder on which the lattice is spread. For contractible polygons, the total power of S_a/S_b, depending on the heights a and b assumed inside and outside respectively, is always one, since the polygon cannot intersect itself. Therefore this polygon contributes the following

factor to the total Boltzmann weight

$$A_{ab}\frac{S_a}{S_b} \tag{B3}$$

in which the result of the δ symbols, ensuring a constant height in the regions immediately inside and outside the polygon is understood. For those polygons that do not have other polygons inside them, the summation on the height assumed in the interior can be performed since it does not appear in the Boltzmann weight otherwise than indicated in (B3). The result is that the weight of the polygon is equal to the largest eigenvalue of A, i.e. Δ. It is important to observe not only that these inner loops all contribute the same factor to the Boltzmann weight, but also that the dependence on b disappears by the summation on a. Therefore the summation on the height assumed in the region immediately surrounding the inner loops can now be performed in the same way, resulting in the same factor for the polygons that surround these regions. This process can be continued for all contractible polygons.

If the lattice is wrapped on a torus, then there may also be polygons that cannot be continuously contracted to a point, because they wind around the torus. These polygons contribute to the Boltzmann weight a factor A_{ab}, depending on the height assumed in the regions on either side of the polygon. These regions themselves also wind around the torus and must be bounded between two non-contractible polygons. Thus the contribution for a total of ℓ such polygons, after the summation on the height assumed in the regions between is performed, is given by $\mathrm{Tr}\, A^\ell$. Now we have obtained a simple expression for the partition sum of the model (B1)

$$Z = \sum_{\text{graphs}} \Delta^p \,\mathrm{Tr}\, A^\ell = \sum_{\Delta'} \sum_{\text{graphs}} \Delta^p \,\Delta'^\ell \tag{B4}$$

in which p and ℓ are the number of contractible and non-contractible polygons, respectively, and the summation on Δ' is over all eigenvalues of A. For a cylinder a similar expression may be derived, in which the matrix product A^ℓ is not traced, but sandwiched between vectors determined by the boundary conditions on the ends of the cylinder. This is applicable only to certain boundary conditions, which forbid the domain walls to terminate on the boundary. It should be noted that these expressions are the same for a wide class of different models, specified only by their adjacency matrix.

B.1. Equivalent Temperley–Lieb model

We now return to the original definition of our model given in equation (5) and write it as a IRF model on the lattice spanned by $\mathcal{L}$ and its dual lattice

$$Z = \sum \prod_{<a,b,c,d>} W\begin{pmatrix} d & c \\ a & b \end{pmatrix}. \tag{B5}$$

If we denote the value of the Potts spins by s and s', and the cases $v = 0$ or $f = 0$ by a big dot ($\bullet$) and $f = 1$ by a small dot ($\cdot$), the weights can, symbolically, be written as

$$
\begin{aligned}
&W\begin{pmatrix} s & \cdot \\ \cdot & s' \end{pmatrix} = W\begin{pmatrix} \cdot & s' \\ s & \cdot \end{pmatrix} = 1 + (\mathrm{e}^{J} - 1)\delta_{s,s'} \\
&W\begin{pmatrix} s & \cdot \\ \cdot & \bullet \end{pmatrix} = W\begin{pmatrix} \bullet & \cdot \\ \cdot & s \end{pmatrix} = W\begin{pmatrix} \cdot & \bullet \\ s & \cdot \end{pmatrix} = W\begin{pmatrix} \cdot & s \\ \bullet & \cdot \end{pmatrix} = \mathrm{e}^{K_1/4} \\
&W\begin{pmatrix} \cdot & s \\ s & \bullet \end{pmatrix} = W\begin{pmatrix} \bullet & s \\ s & \cdot \end{pmatrix} = W\begin{pmatrix} s & \bullet \\ \cdot & s \end{pmatrix} = W\begin{pmatrix} s & \cdot \\ \bullet & s \end{pmatrix} = \mathrm{e}^{J+M_1/4} \\
&W\begin{pmatrix} \bullet & \cdot \\ \cdot & \bullet \end{pmatrix} = W\begin{pmatrix} \cdot & \bullet \\ \bullet & \cdot \end{pmatrix} = \mathrm{e}^{K_1/2+K_2} \\
&W\begin{pmatrix} \bullet & s \\ s & \bullet \end{pmatrix} = W\begin{pmatrix} s & \bullet \\ \bullet & s \end{pmatrix} = \mathrm{e}^{J+M_1/2+M_2}.
\end{aligned}
\tag{B6}
$$

Precisely when we substitute the solution (13), these weights can be written in the form (B1). The eigenvectors of the adjacency matrix that respect the permutation symmetry between the q Potts states, and the corresponding eigenvalues are given by

$$
\begin{aligned}
&\left(\Delta - \frac{1}{\Delta}\right)^2 = q \\
&S = \left(\Delta - \frac{1}{\Delta},\ \Delta^2 - 1,\ \Delta,\ 1\right).
\end{aligned}
\tag{B7}
$$

The eigenvector elements correspond to the states of $\mathcal{A}$ read from left to right in figure B1.

B.2. The central charge and critical exponents

The partition sum (B4) is written as the sum of partition sums of polygon models in which the contractible and non-contractible polygons are weighted differently. It has been noted for a long time that the six-vertex model can also be formulated as a polygon model [8]. The weight Δ of the contractible polygons is related to what is called the crossing parameter, and the weight of the non-contractible loops Δ' can be controlled independently by means of a so called seam [8], which does not affect the free energy. For this class of six-vertex models, which have Boltzmann weights $\{1, 1, 1, 1, (\Delta + 2)^{1/2}, (\Delta + 2)^{1/2}\}$, the central charge has been calculated both numerically and analytically [12, 23]. It has the form

$$
c = 1 - \frac{6k^2}{h(h-1)} \tag{B8}
$$

in which

$$
\Delta = 2\cos\frac{\pi}{h} \qquad \text{and} \qquad \Delta' = 2\cos\frac{k\pi}{h} \tag{B9}
$$

are the weights of the contractible and non-contractible loops respectively. Since the partition sum (B4) is the sum of polygon model partition sums with different values

of c, the central charge of the total corresponds to that of the largest term, i.e. $k = 1$. The other contributions yield the critical exponents of the form

$$x = \frac{k^2 - 1}{2h(h-1)}. \tag{B10}$$

Since Δ and Δ' are two eigenvalues of the adjacency matrix A, Δ satisfies (B7), and $\Delta' \in \{1/\Delta, -1/\Delta, -\Delta, 1, -1\}$. The eigenvalues ± 1 are $(q-1)$-fold degenerate. They give rise to magnetic exponents, since the corresponding eigenvector breaks the permutation symmetry between the q Potts states.

Another possible approach to the critical exponents of the model is to study the long distance dependence of certain two-point correlation functions. In particular for the models defined by (B1) we take an eigenvector of the adjacency matrix

$$\sum_b A_{ab} S'_b = S'_a \Delta' \tag{B11}$$

with an eigenvalue $\Delta' < \Delta$, and study the two-point correlation functions of the operator S'_a/S_a, depending on the local height a

$$\left\langle \frac{S'_{a(0)}}{S_{a(0)}} \frac{S'_{a(r)}}{S_{a(r)}} \right\rangle. \tag{B12}$$

When this correlation is evaluated in the plane, where all polygons are contractible, the prescription is as follows. The polygons that do not include either of the two positions 0 or r, are unaffected and still have, after summation on the interior heights the original weight Δ. The weight of the inner loops that contain either the origin 0 or the site r, normally given by (B3), is now multiplied with the ratio of the eigenvector elements S'_a/S_a. When the summation on the state a in the interior is performed, the polygon acquires the weight Δ', and the modification of the weight, now S'_b/S_b is passed on to the region immediately surrounding this inner polygon. Again the process of summation can be continued. The result is that those polygons that contain precisely one of the positions to be correlated, acquire a factor Δ' instead of Δ.

Finally the polygons surrounding both positions will have a more complicated weight. Let a be the height assumed inside the smallest polygon that surrounds both 0 and r. This height is weighted by a factor S'_a/S_a from each of the operators. The polygon surrounding this region still contributes a weight (B3) which we may write as the (asymmetric) matrix

$$B_{ab} = A_{ab} \frac{S_a}{S_b} \tag{B13}$$

which has the same eigenvalues as A. The summation on the heights assumed in the regions surrounding both 0 and r is in fact equivalent with the matrix multiplication with B. For n such polygons, the end result is therefore some fixed linear combination of the nth power of the eigenvalues of B, and therefore of A. In the thermodynamic limit there will in general be many polygons that surround both points, so that the contribution will be dominated by Δ^n. Correlation functions of this type have been studied in the Coulomb gas approach [11], and decay algebraically as $|r|^{2x}$ with x given by (B10). In this formulation k plays the role of an electric charge.